Advanced Techniques for Characterizing Hydrogen in Metals

CONF-811037--6

DE83 006974

Proceedings of a symposium sponsored by the Corrosion and Environmental Effects Committee of The Metallurgical Society of AIME and the Corrosion and Oxidation Activity of the Materials Science Division of ASM held at the Fall Meeting of The Metallurgical Society of AIME, Louisville, Kentucky, October 13, 1981.

Edited by
N. F. FIORE
Cabot Corporation
Boston, Massachusetts
and
B. J. BERKOWITZ
Exxon Research and Engineering Co.
Florham Park, New Jersey

A Publication of The Metallurgical Society of AIME

1982.

APPLICATIONS OF NUCLEAR REACTION ANALYSIS FOR DETERMINING HYDROGEN AND DEUTERIUM DISTRIBUTION IN METALS

Carl J. Altstetter
Department of Metallurgy and the Materials Research Laboratory
University of Illinois at Urbana-Champaign

One of the most powerful techniques for observing hydrogen isotopes in metals is nuclear reaction analysis. The technique involves the nuclear reaction between the atoms in an energetic particle beam and the hydrogen isotope which is present in the metals. The product particles or radiation are then detected by means of particle counters, solid state nuclear track detectors or radiation counters. The technique has the advantage of being able to detect the lateral distribution in the plane of a flat specimen or the depth distribution normal to the surface. Furthermore, the method is essentially non-destructive, quantitative and sensitive down to the at. ppm concentration range. It is specific to the isotope being studied and therefore relatively free of interferences from solvent or other solute interactions. In this presentation the fundamental characteristics of the technique will be discussed and illustrated using results of recent investigations of deuterium in stainless steel.

Introduction

There are a multitude of reasons for needing information on the hydrogen isotope amount and distribution in metals. One of the chief motivations to determine these quantities is the property changes which are brought about by the presence of hydrogen in metals. Some of these changes are:

a) loss of tensile ductility due to modification of the initiation and growth of microvoids (1)
b) brittle cracking (2)
c) yield and flow stress (3)
d) phase stability (4)
e) physical properties (5) (elastic moduli, superconducting T_c, Curie temperature, resistivity, . . .)
f) blistering and exfoliation (6)

Other authors in this symposium will be discussing some of the above points. Other reasons for studying hydrogen quantities and distributions are for catalysis (7) and corrosion (8), hydrogen storage (9) and plasma contamination in nuclear fusion devices (10). Excellent methods such as X-ray fluorescence and electron spectroscopies are available for analytical metallography of heavier elements, but nearly all of these depend on atomic energy level excitations and thus are not applicable to hydrogen. Consequently, techniques which involve nuclear excitations, de-excitations, decay or scattering fill an important need for chemical characterization of hydrogen isotopes. The nuclear techniques are frequently more suitable than atomic techniques for heavier elements, as well, and deserve to find increased use by metallurgists and materials scientists. Several of the nuclear techniques for hydrogen analysis are characteristic in the sense of characteristic X-ray or electron energies in atomic techniques. This is so for a similar reason: they depend on discrete nuclear energy level transitions. Thus, these nuclear techniques share with SIMS the potential for identification of specific isotopes and thus for hydrogen mapping, in addition to their usability for depth profiling.

No attempt will be made to give detailed descriptions of all of the nuclear techniques and to analyze their good and bad features. Several recent books and symposiums have been devoted to this (11-15). Nevertheless, some perspective is needed on hydrogen analysis by nuclear techniques. In general, one can start with a radioactive species, e.g. tritium, introduce it into a specimen and observe its position by film techniques or its quantity by gamma photon or particle counting. Alternatively, the radioactive element may be produced in situ by particle or photon irradiation to produce a nuclear reaction (transmutation), e.g. $D(d,n)T^*$, with a radioactive product, subsequently identified as above. This is referred to as activation analysis and can be accomplished using activation by neutrons, charged particles or gamma radiation, depending on the element under investigation. It is customary to perform the irradiation and the counting of the radioactive decay product separately, in different pieces of equipment. This requires that the radioactive element have a half-life longer than a few minutes. A large number of nuclear reactions produce excited nuclei which may decay in times far shorter than picoseconds. Such prompt nuclear reactions require that the product particles or radiation be recorded while the exciting radiation is "turned on". One advantage of this is that unless some unwanted reaction has also taken place in the specimen to make it radioactive, the specimens can be handled immediately after irradiation. It is this latter class of prompt nuclear reactions which are considered in this presentation. For the sake of completeness it is noted that elastic and inelastic particle scattering, e.g. α particle scattering, is also a powerful analytical technique. Neutron scattering from hydrogen is widely used for structural determinations and, at high concentrations, radiography, but except for special circumstances (e.g., coincident detection of elastically scattered ions (16) or detection of hydrogen isotopes recoiling from heavy atom impact (17)) scattering of ions from hydrogen is not frequently used. Elastic scattering of ions, also known as Rutherford Ion Backscattering (RIBS) is a very powerful technique often used for detection of heavier atoms, but it is isotope and element non-specific, i.e. does not give rise to a product particle of characteristic energy. Particle energy is conserved and the detected particle is the incident particle. This is not the case for prompt nuclear reaction analysis, as will be seen below.

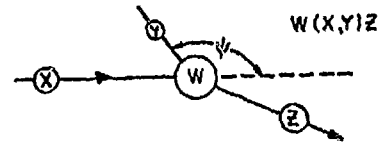

Fig. 1. Projectile atom X undergoes a nuclear reaction with target atom W to produce particles Y and Z.

* The nuclear reaction W(X,Y)Z conventionally denotes irradiation of substance W by X to produce the radiation Y and substance Z, where the radiation could be photons, ions, neutrons or other nucleons.

Prompt nuclear reaction analysis

Consider the nuclear reaction W(X,Y)Z, illustrated in Fig. 1. The total energy is conserved according to equation 1

$$E_X + Q = E_Y + E_Z \qquad (1)$$

where E_i are kinetic energies and Q is the energy decrease or increase due to interconversion of mass and energy according to eqn. 2, the Einstein relation.

$$Q = (m_W + m_X - m_Y - m_Z)\, c^2 \qquad (2)$$

Table 1 cites Q values for nuclear reactions involving hydrogen isotopes. For other elements tables are included in the Nuclear Data (18) and Landolt-Börnstein (19) series. Because the energies involved are so large, the kinetic energy and bonding energy of the target nucleus can be disregarded normally. This means that the technique is not complicated by different states of matter or types of bonding; conversely, bonding information is not obtained as in some of the electron spectroscopies.

Table I. Selected Nuclear Reactions for Hydrogen and Deuterium Analysis

Reaction	Q Mev	σ(max) mb	Beam Energy* Mev
$H(t,n)^3He$	-.8	7540	3.
$H(^6Li,\alpha)^3He$	4.0	270	1.5
$H(^7Li,\gamma)^8He$	17.2	75	2.5
$H(^9Be,d)^8Be$	.6	300	
$H(^{11}B,\alpha)^8Be$	8.59,5.65	420	1.8
$H(^{15}N,\alpha\gamma)^{12}C$	4.96	200	6.5
$H(^{19}F,\alpha\gamma)^{16}C$	8.11	500	16.5
$D(d,p)T$	4.03	90	0.2
$D(d,n)^3He$	3.3	100	0.2
$D(^3He,p)^4He$	18.4	900	0.5
$D(^{10}B,n)^{11}C$	6.5	260	
$D(^{12}C,p)^{13}C$	2.7	250	

(*representative lower limit, laboratory system)

Prompt nuclear reaction analysis, as defined here, is performed in its simplest form by placing a specimen containing the reactive isotope, W, in a beam of particles, X and detecting one or the other of the products, Y or Z of the nuclear reaction. The choice of the nuclear reaction and detected product and the details of the experimental arrangement depend on the hydrogen isotope being analyzed, the equipment available and the requirements of the analysis, e.g. sensitivity, depth or lateral spatial resolution, specificity, etc.

In order for nuclear reaction W(X,Y)Z to be useful for hydrogen isotope analysis the reaction probability must be sufficiently great. The measure of this is the reaction cross section, σ_{XY}, having units of barns (1 barn = $10^{-24}cm^2$). It is related by equation 3 to dN_Y, the number of product Y particles per sec produced when N_X particles per sec impinge on a thin slab, dl, of specimen having density ρ.

$$dN_Y = N_X\, N_W\, \rho\, \sigma_{XY}\, dl \qquad (3)$$

N_W is the number of W target atoms per gram of specimen. It must be emphasized that W is an isotopic species not an elemental species. Frequently ρdl is cited as thickness, ds, in g/cm^2. For quantitative reaction analysis σ_{XY} must be known, so that N_W may be calculated from a measurement of dN_Y with a given analyzing beam current, N_X. For film thickness measurement eqn. 3 is solved for dl or ds. The product particle yield is frequently determined at a given angle, ψ, with respect to the incident beam and in a given angular range, dψ, , so that the differential cross section $\sigma(\psi)$ in cm^2/steradian must be used. For light target atoms the nuclear reaction may arise from a resonant excitation of the target nucleus from a ground state to an excited state. In this case the cross section is a sharply peaked function of projectile energy. It may also be a non-monotonically varying function of detection angle, ψ. For non-resonant reactions the cross section varies more smoothly with projectile energy. If the reaction arises from a resonant excitation of a nucleus there is a threshold energy, below which the cross section is zero, followed by a peak in σ and then a drop off. At higher energies other discrete resonances are possible, with a merger into, effectively, a continuum at higher projectile energies. Fig. 2 shows experimental data and two polynomial fits for the relatively broad excitation function, $\sigma(E_X)$, for the reaction $D(^3He,p)^4He$. Mayer and Rimini have compiled cross section data for other nuclear reactions (15) and Bird (14) has surveyed their use in ion beam analysis.

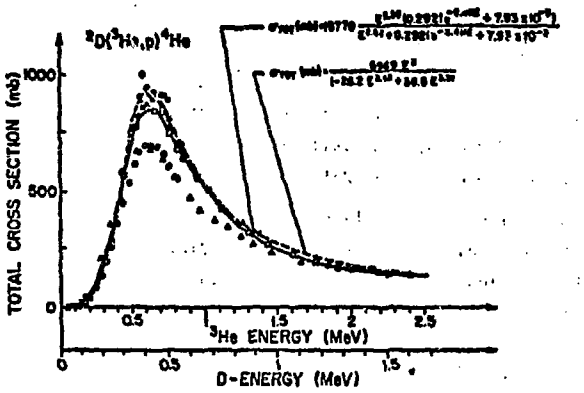

Fig. 2. Nuclear reaction cross section for $D(^3He,p)^4He$ as a function of energy, using either D or ^3He as the projectile atom (25).

The peaked nature of the excitation function gives rise to a useful property of prompt nuclear reaction analysis: the target atoms can be detected only when the projectile energy falls in a band straddling the peak. Since a projectile ion rapidly looses energy as it penetrates the target, it has the proper energy for reaction only within a given depth range inside the material. Thus, by adjusting the initial beam energy, the detection zone can be moved from the surface to depths some microns below the surface. The ramifications of this will now be explored. Consider the schematic representation in Fig. 3, showing the beam impinging on the specimen being analyzed. The incoming particle energy vs. depth relation is plotted, as is the reaction cross section. The interval of energy, ΔE, for reaction corresponds to an interval of distance, Δx, in which the reaction occurs. The depth of this analysis zone below the specimen surface can be selected by controlling the incident particle energy, E_x^0. It should be noted here that because of this property, lack of surface contamination is not crucial to the analysis, and specimen handling and analyzing system gas pressure are not critical. The important material parameter which determines the depth of the analysis zone is the stopping power, $\frac{dE}{dx}$, for the particular particle/target combination. Values of this quantity are tabulated for several projectile ions in all elements (20).

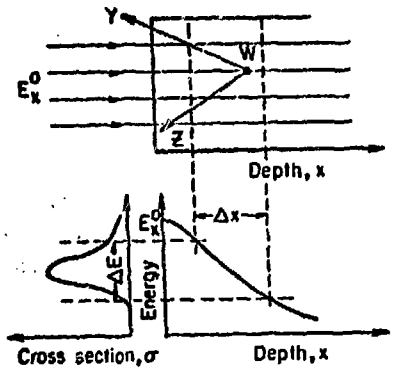

Fig. 3. Schematic design showing the analyzing zone depth for a given projectile energy using the resonance method of depth profiling.

Three basic types of prompt nuclear reaction analysis for hydrogen have been used. The first is for depth profiling, the second is for hydrogen isotope mapping, i.e., for determining isotope distribution in a plane parallel to the surface and the third is for lattice site location using the channeling phenomenon. The first and third types use a silicon barrier detector capable of registering both the number and energies of the product particle, or scintillation media can be used for photon detection. Associated with this detector must be an array of electronic instruments: preamps, amplifiers, multichannel pulse height analyzers, power supplies and digital recording and computation capability. As will be described and illustrated shortly, such a measurement system can give hydrogen isotope depth profiles with excellent depth resolution (10nm in favorable cases) (21) and sensitivity (1 at. ppm) (22). It is generally, but not universally, conducted with the detector on the incident beam side of the specimen. The hydrogen isotope mapping technique utilizes a solid state nuclear track detector film for registering the product particles which pass through the specimen (23,24). This scheme has just recently been demonstrated for use with metal targets, and it promises to yield reasonable lateral resolution (1μm) and sensitivity (25,26). This detection scheme requires only an expendable plastic film costing a few cents. Electronic detection of particles can also yield isotope maps by utilizing a finely focused excitation beam and rastering it across the specimen in the manner of electron beam microprobe techniques (27).

Hydrogen isotope depth profiling

Many studies and several conferences have explored the use of surface barrier detectors for hydrogen isotope depth profiling (13-15). Chu, Mayer and Nicolet have recently compiled a very useful bibliography for backscattering spectroscopy, and in it are cited conference proceedings dealing with the use of ion beams for all types of analysis (11). Deconninck's book is required reading for anyone entering the field of radioanalytical physics (12). Böttiger et al have reviewed light isotope profiling (22) and Ziegler et al (21) is a report of a round robin analysis of hydrogen or deuterium in silicon. Picraux has recently surveyed the use of nuclear reaction analysis for hydrogen analysis (28). All of these references provide ready access to the depth profiling literature.

Fig. 4 shows a typical experimental set up for depth profiling. The incident beam enters from the accelerator at the left with an energy appropriate to the nuclear reaction being utilized (see Table I). It is steered through defining and collimating apertures to the specimen. The product particles may or may not be filtered or mass analyzed before reaching the detector, which is placed at a precisely known angle to the incident and specimen surface and subtends a precisely known solid angle. The Faraday cup, specimen current meter and intermittently introduced incident beam scatterer are necessary to make quantitative absolute measurements of isotope content

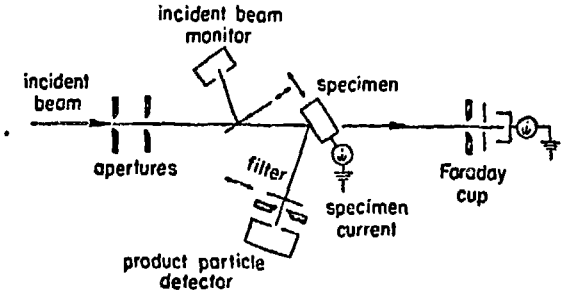

Fig. 4. Experimental arrangement for depth profiling by nuclear reaction analysis.

through the use of equation 3, suitably modified to include geometrical factors. Silicon implanted with ^{1}H, ^{2}H or ^{3}H makes a suitable calibration standard because it is known to capture and retain 100% of the implanted ions up to doses of 10^{17}atoms/cm^2 (21,29) provided that the surface does not spall due to too shallow implantation (E < 10kev) or too high a fluence (>10^{17}cm^{-2}).

Two depth profile analysis techniques can be used. The so-called resonance method utilizes the principle illustrated in Fig. 3. Product particle counts are made for time intervals at successively higher primary beam energies, E_x^0. The depth resolution, Δx, is controlled largely by the width of the resonance and the stopping power of the target material. This method yields good sensitivity and large depth range, with good depth resolution when the resonance is sharp. It is fairly rapid because the product particles are not energy analyzed. In the energy analysis method the beam energy is fixed, thus determining the analysis zone location. The energy of the product particle is analyzed with a multichannel pulse height analyzer to give N(E), the number of product particles in a given narrow energy increment. The conversion of this information to a concentration depth profile can be simply made for high Q reactions where the product particle energy is largely determined by Q and not by E_x (cf. equation 1). Thus, to a first approximation, regardless of where the target nucleus was in the detection zone, each product particle is born with an energy characteristic of a transition between nuclear quantum states. As the particle travels out of the material it loses energy, according to the stopping power of the specimen. Thus the most energetic particles detected come from the material closest to the surface, and less energetic particles were born at target nuclei deeper inside the specimen and lost energy as they traveled to the surface. Obviously the depth resolution in this method of analysis is very sensitive to the resolving power and placement of the detector as well as having a sufficiently large stopping power of the specimen so that a large energy difference arises from a small difference in path length. In order to obtain reasonable statistical accuracy in the N(E) distribution, long (up to several hours) counting times are used. Protons and neutrons are generally not suitable for this analysis mode due to the small stopping power of most metals for these particles.

Prompt ion-induced autoradiography

Mapping of hydrogen isotope distribution with a solid state nuclear track detector (SSNTD) is done using prompt ion-induced autoradiography (PIIA), illustrated in Fig. 5 (25,26). The specimen is a foil whose thickness must be great enough (~ 10μm for Fe) to stop the primary beam. Failing this, filters may be used between the specimen and the SSNTD. The more energetic product particles (when Q > 0) pass out of the specimen and through the SSNTD, leaving damage tracks. These are subsequently developed into deep pits or holes by etching the SSNTD under controlled conditions of time, temperature and reagent concentrations. For many purposes inorganic materials are useful SSNTD's (23,24), but for PIIA a cellulose nitrate film works well. In LR115 type II+, for example, a 12μm thick, red-dyed cellulose nitrate layer is supported on a durable 100μm Estar base. Upon development, a hole in the red layer is created. Shining green light from behind the SSNTD reveals a pattern of bright spots on a black background. These can be quantified using an analytical optical microscope system (Quantimet, for example) or by spark counting or enhancement equipment (23,30). With a proper choice of beam energy and current, specimen thickness, exposure time and etching conditions the distribution of tracks will represent the distribution of target nuclei in a plane parallel to the surface and at the depth of the analysis zone. Total concentrations within the zone are derivable from the average track density.

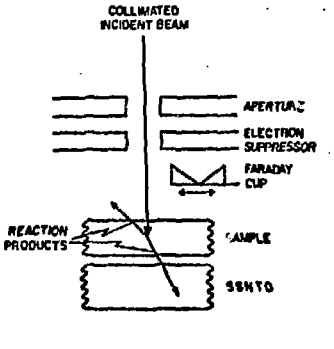

Fig. 5. One experimental arrangement for prompt ion-induced autoradiography.

+ available from Kodak Pathé, Paris, France.

SSNTD's are essentially insensitive to light, allowing them to be handled without difficulty. Materials are being developed with sensitivity to different particles, so that a variety of nuclear reactions can be used for PIIA. In principle other detection methods are usable such as gamma sensiti emulsions or scintillation material and channel plates for direct imaging.

Interstitial site location

In single crystals a collimated beam of ions can travel between rows or between planes of atoms with the probability of interaction with the atoms located on the crystal lattice sites decreased compared with a random direction. However, these "channeled" atoms can interact more strongly with atoms located on the interstitial sites which are located within the channels. When the interaction is a nuclear reaction between the target and projectile atoms, energetic product particles or photons can be detected and their numbers correlated with those expected for various alternative site occupancies. The experiment requires beam collimation to better than one degree and a precise specimen goniometer, since channeling behavior dominates only when the beam is within a few degrees of the channeling direction. By monitoring both the product particles and backscattered incident particles as a function of beam incidence angle the location of the interstitial atoms relative to the lattice atoms may be determined for that channeling direction. By repeating the measurements for other crystallographic directions it is possible to exclude some of the site alternatives and deduce the interstitial atom site location. A further use of the technique is to assess changes in perfection of the crystal resulting from ion bombardment damage. Discussion of the application of the technique will not be made. The work of Picraux and co-workers (31,32,33) demonstrates the power of the technque for hydrogen and deuterium site location.

Applications

Chu, Mayer and Nicolet's book, (11) "Backscattering Spectrometry", has a carefully prepared bibliography on ion beam analysis techniques including citations up to 1978 of books and conference proceedings, many of which contain material on applications of nuclear reaction analysis. They also include a bibliography on hydrogen and helium in metals. In addition, several papers on nuclear reaction analysis for hydrogen were included in a recent conference in Aarhus, Denmark (13). The literature on nuclear reaction analysis for hydrogen using ion beams is not large, perhaps numbering several dozen papers. Consequently, one cannot at this point speak of standard

techniques for analysis of hydrogen and deuterium. A few examples will be given, without attempting to cite all the recent, excellent work in the field.

Deuterium is a very useful isotope for analysis, since it acts chemically very similarly to hydrogen, though it diffuses more slowly. It is far easier to handle and cheaper than tritium, and has the advantage over hydrogen that it is not naturally present in specimens or on their surfaces. The Plasma-Wall Interaction group at the Max Planck Institut für Plasmaphysik* has used the $D(^3He,p)^4He$ reaction to advantage for both D and ^3He analysis. Their experimental arrangement is basically that of Fig. 3 using a 3Mev van de Graaff accelerator and with the added capability of specimen cooling, in situ ion implantation and Auger electron or X-ray detection. One of the objectives of the Garching group has been to understand light isotope implantation, trapping, blistering and reemission from the first wall material of a fusion reactor. Stainless steel (29,34-36), graphite (37), and molybdenum (38) are among the structural materials studied. Groups at Sandia National Laboratory, University of Aarhus and other laboratories have also exploited the $D(^3He,p)^4He$ reaction for depth profiling of metals, ceramics and polymers. Fig. 2 shows the estimated total cross section vs ^3He energy for the $D(^3He,p)^4He$ reaction. A relatively low resonance energy and high Q value, table I, means that the product particles (~3Mev α, ~15Mev p) can be easily distinguished from the incident particles (0.5 - 3.0Mev ^3He). Also the product particle energies are relatively less affected by incident particle energy than some of the other nuclear reactions used (28). Typical results are shown in Fig. 6 for deuterium in AISI 316 stainless steel. These depth profiles were determined by the energy analys , technique. Different quantities of deuterium were introduced by implantation using 14kev D_2^+ ions, yielding 7kev D at the specimen surface. The specimen was cooled to 153K. It is important in hydrogen isotope analysis that specimen temperature be maintained at such a temperature or lower, otherwise significant movement and loss of hydrogen from the analysis zone will occur. This is particularly important for low energy hydrogen implanted specimens, where the concentration gradients can be extremely high. Cathodic and thermal charging of hydrogen may be less severe, but nuclear reaction analysis is a near-surface technique, and loss of hydrogen through the surface must be recognized (39). Note the extremely high concentration of deuterium (Fig. 6) which can be produced by ion implantation to fluences representative of those expected for the first wall of a fusion reactor.

* Garching, West Germany.

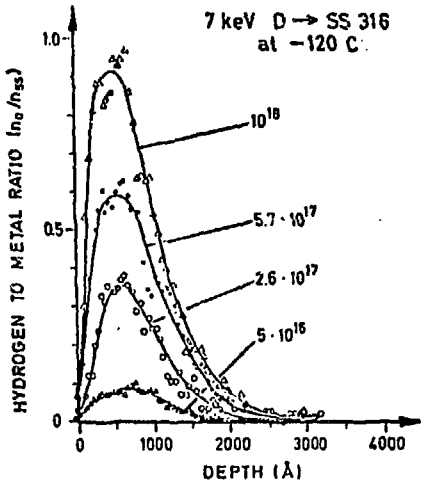

Fig. 6. Deuterium depth profiles determined by energy analysis of ^4He product particles from the $D(^3He,p)^4He$ reaction. Various fluences (atoms/cm^2) of 7kev deuterium implanted in AISI 316.

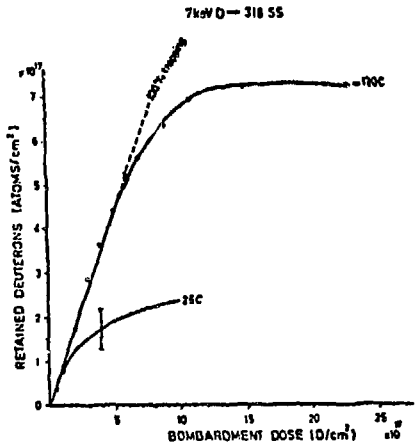

Fig. 7. Total deuterium remaining in AISI 316 specimen implanted with increasing doses of 7kev deutrons at two different temperatures. Analysis made by counting proton yield from the $D(^3He,p)^4He$ reaction using a 0.79Mev beam of $^3He^+$ (34).

Other problems which are inherent in the technique are that although for many purposes it is "non-destructive", still the analyzing beam creates atomic disp acement damage and subsequent trapping (40), enhanced diffusion during irradiation (29,41) and, when the specimen is thick enough to stop the analyzing beam, a build-up of these atoms occurs in the target. This effect may be ameliorated to some extent by the fact that the cross section falls precipitously at ^3He energies below 500kev so that the ^3He comes to rest outside the analyzing zone when using the energy analysis method. When the projectile and target atoms are the same isotope, e.g. for D(d,p)T, there are obvious problems of contamination by the analysing beam. Beam heating of the specimen can also be a problem requiring care in maintaining good thermal contact between the specimen and specimen holder, particularly when foil specimens are used. Note that a typcial analyzing beam current of 1μA/cm^2 gives a thermal loading of 1W/cm^2 with a 1Mev beam.

The energy analysis method is relatively time consuming because for good depth resolution, ten or so nm, the detector must subtend a small angle (a few $x10^{-4}$sr) and its energy discrimination and the energy increment in the N(E) distribution should be small. The detector placement also influences depth resolution (42), with small angles to the surface increasing resolution, but giving rise to problems with surface roughness, specimen placement, stability of placement, multiple scattering, straggling and the possibility of changes due to blistering or to sputtering of the surface by the analyzing beam. Oblique incidence of the analyzing beam can also increase resolution in the near-surface region (43,44). As with many techniques, there is a trade-off between resolution and sensitivity. The high energy protons produced in the $D(^3He,p)^4He$ reaction are very penetrating and by counting them with a relatively wide angle detector, a measure of the total amount of deuterium in the analyzing zone may be obtained in a few minutes. This proton count can be used as a check on the area under the N(E) distribution of the product α particles. Examples of the use of total counts of protons are the determinations of the retention of implanted deuterium Fig. 7, (29), replacement of deuterium by hydrogen or helium (36,45) and determination of the diffusion co-efficient of deuterium (35).

A limitation of the energy analysis technique of profiling arises from the sharpness of the peak in reaction cross section for resonance reactions. This gives an effective analysis zone for the $D(^3He,p)^4He$ reaction of only a μm or so in first period transition elements and less in heavier metals with greater stopping power. This is not a serious limitation for low energy implantation studies, but may be detrimental for depth profiling of thermally or cathodically charged specimens having deeper penetration of deuterium. Analysis at depths up to ten or more μm can be done by detecting protons and using the resonance technique, though for the relatively broad $D(^3He,p)^4He$ resonance the depth resolution is not good. The proton counts vs incident particle energy, E_x^o, raw data is converted to deuterium concentration vs depth information by deconvolution, requiring accurate values of reaction cross section vs E_x for accurate depth determination. Deconvolution techniques are described by Lewis (46) and others (29,47).

Other convenient nuclear reactions involving deuterium are the $D(d,p)T$ non-resonant reaction, which has a Q value of 4.03 and the $D(d,n)^3He$ with a Q value of 3.3Mev. The Ruhr University* group has used the former reaction for deep probing of implanted deuterium (44). A deuterium probe has the advantage that the deuterium travels deeper into the material at a given incident energy, and the deuterium undergoes a nuclear reaction at relatively low energy (< 100kev). Thus, the analysis zone can be more than 10μm deep with an initial energy of 2Mev (44). The depth resolution becomes considerably poorer, nearly 0.5μm, due to energy and angular straggling, but for analysis of total content this would not be a problem. The Oak Ridge National Laboratory group has used the $D(d,p)T$ reaction for depth profiling in metals and oxides and to determine diffusion co-efficients (39,41,48). They have clearly demonstrated that although nuclear reactions may occur with other solutes (e.g. ^{12}C and ^{16}O) in the metal, these reactions do not interfere with the deuterium analysis, and they can even be utilized for simultaneous analysis of these species.

The $H(^{19}F, \alpha\gamma)^{16}O$ and $H(^{15}N, \alpha\gamma)^{12}C$ reactions have both been used for hydrogen analysis, but in these cases the γ radiation rather than the α particle has been detected. This is due to the convenience of placing the γ detector outside the specimen chamber, whereas the α detector must be inside the chamber. These reactions each have a multiplicity of sharp resonances so that the resonance analysis technique provides good depth resolution (~ 25nm for ^{19}F and 6nm for ^{15}N at the surface of Si (20)). Unfortunately, the heavier ions are more readily stopped in the specimen so that the depth of analysis is limited. If higher initial ion energies are used, other resonances may be excited in H or in other elements, and analysis becomes more complicated. Another drawback is the contamination layer containing H, almost invariably present on the surface of specimens. The high incidence energies (> 6Mev) also place a more stringent requirement on the ion accelerator. Clark et al (49) compare the relative merits of the two nuclear reactions and apply them to the analysis of H in Si, SiO_2 and Au. The ^{19}F reaction was used in an early application of prompt nuclear reaction analysis in the detection of H in lunar rocks (50). A very recent use of this reaction was for hydrogen trapping studies in Mo (51). More about the use of the ^{15}N reaction will be presented in this symposium (52). Gamma detection is also performed with the $H(^7Li,\gamma)^8Be$ reaction, also to be illustrated in a presentation at this symposium (53).

Different detection technique is required in the $H(t,n)^3He$ and $D(t,n)^4He$ reactions, where the product neutron is detected either with or without coincident He ion detection. In these non-resonant reactions the neutron energy varies with the incident particle energy, thus the energy analysis method must be used. The neutrons loose little energy in passing through the specimens so that they can be detected at either the back or the

* Institut für Experimentalphysik, Bochum, West Germany.

front of the specimen. The potential for obtaining depth profiles at great depths (> 10μm) within the target are lost due to the relatively poor resolution of neutron time of flight spectrometry and straggling of the incident beam at great depths. Interference from other (t,n) reactions and from the contamination layer on most specimens give serious limitations on detection sensitivity (1000 ppm H in a high Z material) (54). It must be noted that neutron production using light ion beams could be a serious safety problem, particularly in the absence of neutron yield data for a wide variety of experimental conditions (55).

In principle many other nuclear reactions with D or H are possible using light ion beams. Of the analysis beam elements not yet discussed here the $H(^{11}B,\alpha)^{8}Be$ reaction used by the Grenoble group deserves notice (56,57). This reaction has the advantage of a reasonably high resonance cross section at a relatively low ^{11}B energy (1.79Mev). Furthermore, B^{+}beams can be produced easily from RF excited ion sources using borane, and ^{11}B is the most abundant naturally occurring isotope of boron. The surface contamination problem is still troublesome at low hydrogen concentration in the specimen. A strong resonance at 6.6Mev overlaps the weaker 1.79Mev resonance, making deep profiles difficult. Other possible reactions using C, O and Be isotope beams have not been exploited for H and D analysis, though there are several promising reactions with reasonable Q values and cross sections. Other hydrogen and deuterium detection techniques involving elastic and quasi-elastic scattering of protons or deuterons (16,21,58) will not be discussed, nor will the elastic recoil detection (ERD) technique involving detection of the recoiling H or D due to heavy ion scattering (e.g. Cl). Doyle and Peercy have compared ERD with nuclear reaction analysis (16). This technique becomes similar to SIMS at low bombardment energies, but at higher energies is able to probe more deeply.

Since only a limited study has been reported (25,26) for analysis of a hydrogen isotope in metals by PIIA, the results will be briefly described. Possible future applications will be indicated. The use of SSNTD's is not new for nuclear reaction analysis. It was first discussed in 1965 by Malmon for biological material analysis, but the report in the Journal of Theoretical Biology apparently did not reach many materials scientists (59). In the present experiments deuterium was introduced either by electrolytic charging into the metal or else in the form of deuterated phthalic acid crystals left after a droplet of phthalic acid solution in D_2O evaporated from the surface of the metal specimen. In the former case one-half of a 6μm thick Hastelloy G

specimen* was masked during charging and the interface between the charged and uncharged regions was imaged by PIIA, Fig. 8, using the $D(^{3}He,p)^{4}He$ reaction. The nuclear tracks caused by the alpha particles appear as bright dots, clearly showing that the deuterium was localized to the left half of the foil. The indication of a small quantity of deutrium on the other half may be due to the presence of adsorbed deuterium. The autoradiograph was taken with a 400 na beam of $^{3}He^{+}$ at 0.63 Mev for 137 seconds, yielding a total analysing fluence of 6.9×10^{14} $^{3}He/cm^{2}$. In this particular detector film the tracks were etched to a maximum diameter of 10μm. This factor plus geometrical factors concerned with analyzing zone depth, specimen thickness and product particle range determine the lateral resolution and sharpness of the resulting autoradiography. This is illustrated in Fig. 9, which compares an optical micrograph of deuterated phthalic acid crystals with the ion induced radiograph recorded at the opposite face of the 6μm thick Hastelloy G specimen. The general features of the optical micrograph are reproduced, e.g. the curvature of the droplet and the clustering of crystals. It is estimated that resolution of the order of 1um is possible through optimization of the experimental conditions. The exact quantity of deuterium present in or on the specimens in Figs. 8 and 9 is not known precisely. It is estimated from other experiments that there may have been 2-3 thousand at. ppm of deuterium dissolved in the specimen for Fig. 8. Further experimentation is underway to establish the level of detectability of deuterium using PIIA. Calculations based on available data indicate an ability to detect less than 1 at. ppm. Since deuterium diffuses out of the specimen at room temperature it is necessary that the specimens be refrigerated immediately after charging or implanting and be kept refrigerated during analysis.

If the promise of the initial PIIA study is realized, a number of applications are suited to the resolution and sensitivity of PIIA. For example, the location of deuterium at optical microscopic scale trap sites (particle interfaces, grain boundaries, precipitates) can be imaged, and distribution of deutrium among the matrix, these trap sites and more macroscopic features such as crack tips and welds can be studied, hopefully resulting in better understanding of hydrogen embrittlement. It should not be difficult to investigate specimens under stress. Back emission techniques could prove useful in determining average concentration in the near surface region of bulk specimens (26). PIIA is not limited to the $D(^{3}He,p)^{4}He$ reaction for hydrogen isotope detection, nor is it limited to hydrogen isotope detection. The ease and economy of PIIA plus some of the unique capabilities

* Donated by N. Fiore of Notre Dame University.

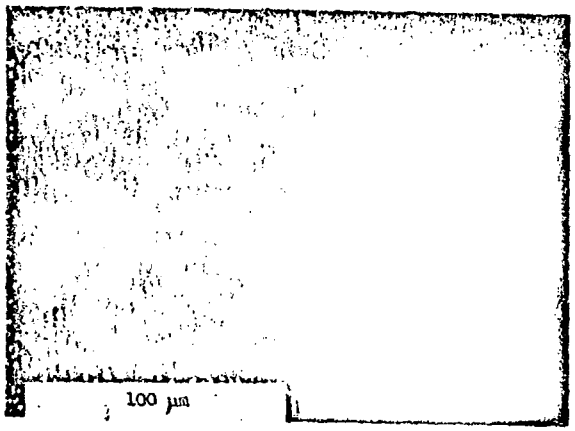

Fig. 8. Prompt ion-induced autoradiography of 6μm Hastelloy G specimen deuterated on the left hand side by cathodic charging. D(^{3}He,p)^{4}He reaction used with ^{4}He detected in LR115 type II SSNTD. 400na beam of $^3He^+$ at 0.63Mev for 137 seconds (25).

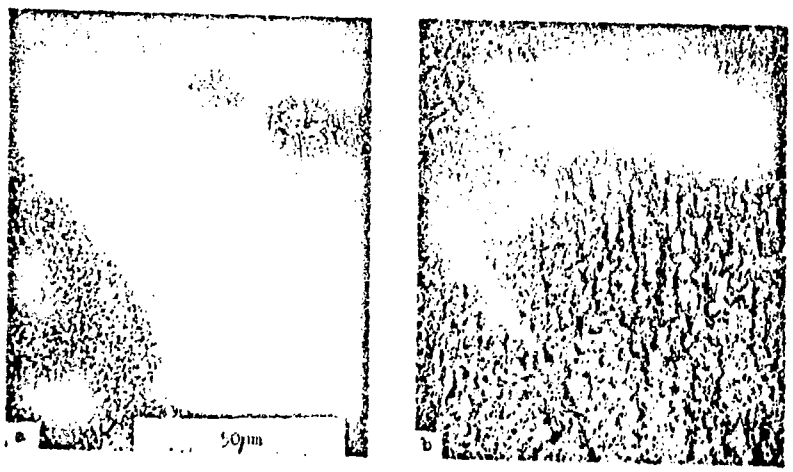

Fig. 9. a) prompt ion-induced autoradiograph b) optical micrograph of deuterated phthalic acid crystals deposited on the surface of a 6μm Hasteiloy G foil. LR115 type II SSNTD was placed at the opposite face of the foil (25).

should allow its use in a variety of practical applications. Development of new SSNTD materials with greater sensitivity and selectivity is to be expected (60).

Summary

The use of ion beams for materials analysis has made a successful transition from the domain of the particle physicist to that of the materials scientist. The subcategory of this field, nuclear reaction analysis, is just now undergoing the transition, particularly in applications to hydrogen in materials. The materials scientist must locate the nearest accelerator, because now he will find that using it can solve mysteries that do not yield to other techniques.

Acknowledgement

This research was supported by the Department of Energy under contract DOE-EY-76-C-02-1198 administered through the Materials Research Laboratory and by the National Science Foundation under contract NSF-DMR-77-09808. The efforts of Mr. Scott Gatfield in helping with the literature survey are greatly appreciated. Thanks are also due the University of Illinois for their policy of granting sabbatical leave - a time to poke your head up out of the rut and see what's happening in other places and other fields. The vigor and expertise of the analysis group at the Max Planck Institut für Plasmaphysik in Garching were instrumental in the initiation of this work. Their hospitality and support during my sabbatical leave there are noted, with pleasure. Mr. R. Ilic's enthusiasm and knowledge of solid state nuclear track detectors came at an important time in this work on nuclear reaction analysis. His role is gratefully acknowledged.

References

1. A. W. Thompson, Effect of Hydrogen on Behavior of Materials, A. Thompson and I. Bernstein, eds., AIME, New York, 1976, p. 467.
2. R. P. Wei, Hydrogen Effects in Metals, A. Thompson and I. Bernstein, eds., AIME, Warrendale, Pa., 1981, p. 677.
3. H. Kimura, H. Matsui and T. Kimura, Trans. Jap. Inst. Met. 21 (1980), p. 533.
4. H. K. Birnbaum, Environment-Sensitive Fracture of Engineering Materials, Z. Foroulis, ed., AIME, Warrendale, Pa., 1979, p. 326.
5. G. Alefeld and J. Vokl, Hydrogen in Metals I and II, Springer Verlag, Berlin, 1978.
6. S. K. Das and M. Kaminsky, J. Nucl. Mat., 53 (1974) p. 115.
7. M. W. Roberts and C. S. McKee, Chemistry of the Metal-Gas Interface, Oxford University Press, Oxford, 1978.
8. D. Vaughn, D. Phalen, C. Peterson and W. Boyd, Corrosion 19 (1963) p. 315.

9. M. Kesten and K. Windgassen, Hydrogen Effects in Metals, A. Thompson and I. Bernstein, eds., AIME, Warrendale, Pa., 1981, p. 1017.
10. R. Behrisch, Nuclear Fusion 189 (1978) p. 1315.
11. W. Chu, J. Mayer and M. Nicolet, Backscattering Spectrometry, Academic Press, New York, 1978.
12. G. Deconninck, Introduction to Radioanalytical Physics, Elsevier Scientific Publ. Co., Amsterdam, 1978.
13. Proceedings of Aarhus Conference on Ion Beam Analysis, H. Anderson, J. Böttiger and H. Knudsen, eds., Nucl. Instr. Meth. 168 (1980).
14. J. R. Bird, B. L. Campbell and R. J. Cawley, Prompt Nuclear Analysis Bibliography to 1976, AAEC/E443, Australian At. Energy Comm. (1978).
15. J. Mayer and E. Rimini, Ion Beam Handbook for Materials Analysis, Academic Press, New York, 1977.
16. B. L. Doyle and P. S. Peercy, Appl. Phys. Lett. 34 (1979) p. 811.
17. O. N. Jarvis and A. C. Sherwood, Nucl. Instr. Meth., 115 (1974) p. 271.
18. A. H. Wapstra and N. B. Gove, Nuclear Data Tables, 9A, No. 4-5, 1971.
19. Landolt-Börnstein, New Series, Vol. 5, part b, Springer Verlag, Berlin, 1973.
20. J. F. Ziegler, The Stopping Power and Range of Ions in Matter, Vols. 3-6, Pergamon Press, Oxford, 1980.
21. J. F. Ziegler et al., Nucl. Instr. Meth. 149 (1978) p. 19.
22. J. Böttiger, S. T. Picraux and N. Rud, Ion Beam Surface Layer Analysis, O. Meyer, G. Linker and F. Käppler, eds., Plenum Press, New York, 1976, p. 811.
23. R. L. Fleischer, P. B. Price and R. M. Walker, Nuclear Tracks in Solids, U. of Cal. Press, Berkeley, 1975.
24. H. Francois, Solid State Nuclear Track Dectectors, Pergamon Press, Oxford, 1980.
25. R. Ilić and C. Altstetter, Nucl. Instr. Meth. 185 (1981) p. 505.
26. C. Altstetter and R. Ilić, Int. Conf. on Solid State Nuclear Track Detectors, Bristol, Sept. 1981.
27. G. M. Padawer, D. J. Larson and P. N. Adler, Met. Trans. 2 (1971) p. 2287.
28. S. T. Picraux, Physics Today, October 1977, p. 42.
29. C. J. Altstetter, R. Behrisch, J. Böttiger, F. Pohl and B. M. U. Scherzer, Nucl. Instr. Meth. 149 (1978) p. 59.
30. M. Najžer, R. Ilić and I. Remec, Solid State Nuclear Track Detectors, H. Francois, ed., Pergamon Press, Oxford, 1980, p. 363.
31. S. T. Picraux and F. L. Vook, Applications of Ion Beams to Metals, S. T. Picraux, E. P. EerNisse and F. L. Vook, eds., Plenum Press, New York, 1974, p. 407.
32. S. T. Picraux and F. L. Vook, Ion Implantation in Semiconductors, Plenum Press, New York, 1975, p. 355.
33. S. M. Myers, S. T. Picraux and R. E. Stoltz, J. Appl. Phys., 9 (1979) p. 5710.
34. C. J. Altstetter, R. Behrisch and B. M. U. Scherzer, J. Vac. Sci. Techn. 15 (1978) p. 706.
35. W. Möller, B. M. U. Scherzer and R. Behrisch, Nucl. Inst. Meth. 168 (1980) p. 289.
36. R. S. Blewer, R. Behrisch, B. M. U. Scherzer and R. Schulz, J. Nucl. Mat. 76 and 77 (1978) p. 305.
37. B. M. U. Scherzer, R. Behrisch, W. Eckstein, V. Littmark, J. Roth and M. K. Sinha, J. Nucl. Mat. 63 (1976) p. 100.
38. R. Schulz, R. Behrisch and B. M. U. Scherzer, J. Nucl. Mat. 93 and 94 (1980) p. 398.
39. M. Lewis and K. Farrell, Hydrogen Effects in Metals, I. Bernstein and A. Thompson, eds., AIME, Warrendale, Pa., 1981, p. 159.
40. S. M. Myers, S. T. Picraux and R. E. Stoltz, Hydrogen Effects in Metals, I. Bernstein and A. Thompson, eds., AIME, Warrendale, Pa., 1981, p. 87.

41. M. B. Lewis, J. Nucl. Mat. 88 (1980) p. 23.
42. W. Eckstein, R. Behrisch and J. Roth, Ion Beam Surface Layer Analysis, O. Meyer, G. Linker and F. Käppeler, eds., Plenum Press, New York, 1976, p. 821.
43. P. P. Pronko and J. G. Pronko, Phys. Rev. B, 9 (1974) p. 2870.
44. M. Hufschmidt, W. Möller, V. Heintze and D. Kamke, Ion Beam Surface Layer Analysis, O. Meyer, G. Linker and F. Käppeler, eds., Plenum Press New York, 1976, p. 831.
45. B. L. Doyle, W. R. Wampler, D. K. Brice and S. T. Picraux, J. Nucl. Mat. 93 and 94 (1980) p. 551.
46. M. B. Lewis, ORNL/TM-6697, Oak Ridge National Laboratory, 1979.
47. V. L. Whitton, I. V. Mitchell and K. B. Winterbon, Can. J. Phys. 49 (1971) p. 1225.
48. M. B. Lewis and K. Farrell, Advanced Techniques for Characterization of Microstructures, J. Spitznagel and F. Wiffen, eds., AIME, Warrendale, Pa., 1981.
49. G. J. Clark, C. W. White, O. O. Allred, B. R. Appleton, F. B. Koch and C. W. Magee, Nucl. Instr. Meth. 149 (1978) p. 9.
50. D. A. Leich and T. A. Tombrello, Nucl. Instr. Meth. 108 (1973) p. 67.
51. A. L. Hanson, D. H. Vincent and C. N. Davids, J. Nucl. Mat. 98 (1981) p. 259.
52. W. A. Lanford, Advanced Techniques for the Characterization of Hydrogen in Metals, N. Fiore, ed., AIME, Warrendale, Pa., 1982.
53. R. L. Schulte and P. N. Adler, Advanced Techniques for the Characterization of Hydrogen in Metals, N. Fiore, ed., AIME, Warrendale, Pa., 1982.
54. J. C. Davis and J. D. Anderson, J. Vac. Sci. Techn., 12 (1975) p. 358.
55. J. R. Bird, Nucl. Instr. Meth. 168 (1980) p. 85.
56. E. Ligeon and A. Guivarc'h, Rad. Eff. 27 (1976) p. 129.
57. E. Ligeon, A. Guivarc'h, J. Fontenille, M. Le Contellee, R. Danielou and J. Richard, Nucl. Instr. Meth. 168 (1980) p. 499.
58. R. S. Blewer, Appl. Phys. Lett. 23 (1973) p. 593.
59. A. G. Malmon, J. Theor. Biol. 9 (1965) p. 77.
60. S. P. Ahlen, P. B. Price and G. Tarlé, Physics Today, September 1981, p. 32.